

Crystal structure and specific heat of GdCuGe

Sudhindra Rayaprol*, C. Peter Sebastian, Rainer Pöttgen

Institut für Anorganische und Analytische Chemie and NRW Graduate School of Chemistry, Westfälische Wilhelms-Universität Münster, Corrensstraße 30, 48149 Münster, Germany

Received 18 January 2006; received in revised form 28 March 2006; accepted 2 April 2006
Available online 2 May 2006

Abstract

A single crystal study of GdCuGe revealed full copper–germanium ordering: NdPtSb type, space group $P6_3mc$, $a = 423.2(1)$, $c = 753.7(2)$ pm, $wR_2 = 0.0443$, 414 F^2 values and 10 variables. The copper and germanium atoms build up two-dimensional networks of ordered $[\text{Cu}_3\text{Ge}_3]$ hexagons with Cu–Ge distances of 244 pm. Consecutive $[\text{Cu}_3\text{Ge}_3]$ layers are rotated by 60° around the perpendicular c -axis with respect to each other. The $[\text{Cu}_3\text{Ge}_3]$ hexagons show a weak puckering. Heat capacity measurements on the polycrystalline sample of GdCuGe establishes antiferromagnetic ordering around 14 K in agreement with reports in the literature. The curves of heat capacity measured in different applied fields crosses each other at two well-defined points exhibiting a behavior usually associated with heavy fermion compounds. The results of the structural analysis and heat capacity measurements are discussed in the light of these interesting observations for a gadolinium intermetallic.

© 2006 Elsevier Inc. All rights reserved.

Keywords: A. Gadolinium germanide; C. Crystal structure; D. Specific heat

1. Introduction

Ternary equiatomic intermetallics $RETX$, where RE = rare earth element, T = transition metal and X = element of the 3rd, 4th or 5th main group, are being extensively studied as they exhibit anomalous physical and magnetic properties. Overviews on the crystal chemistry and outstanding properties of these materials can be found in various review articles [1–4, and ref. cited therein]. Among the ternary rare-earth intermetallics, the ones with gadolinium (with deeply localized f orbitals) have been found to exhibit a large variety of magnetic and physical phenomena, such as ferromagnetic ordering, antiferromagnetism, negative magnetoresistance, large magnetocaloric effect, etc. [5–10]. Several gadolinium intermetallics, such as Gd_2PdSi_3 or Gd_2CuGe_3 exhibit a resistivity minimum before the ordering temperature as seen in Kondo lattices, however without signatures of any Kondo-type interactions [11]. Another unusual behavior, which motivated

systematic investigations on the physical properties of gadolinium intermetallics has been the observation of heavy-fermion-like heat-capacity anomalies [9]. Several gadolinium intermetallics, crystallizing with hexagonal structures of the type AlB_2 , ZrNiAl , MgZn_2 , etc. exhibit interesting electrical and magnetic properties [1,12,13]. Therefore, in order to have a better understanding of such unusual behavior of gadolinium intermetallics, there is an urgent need to explore new gadolinium intermetallic systems to have a broader experimental evidence for proper theoretical approach in this direction.

The equiatomic germanide GdCuGe [14] is known to order antiferromagnetically with a Néel temperature of 17 K [1,15–18]. ^{155}Gd Mössbauer spectroscopic measurements also establish the magnetic transition around 17 K [19]. In all previous studies [16,19], the AlB_2 structure with a statistical distribution of copper and germanium on the boron network was assumed on the basis of X-ray powder diffraction. Herein we report a single crystal study and confirm the copper–germanium ordering. Furthermore, we report on the unusual heat capacity behavior of GdCuGe.

*Corresponding author. Fax: +49 251 833 6002.

E-mail address: rayaprol@gmail.com (S. Rayaprol).

2. Experimental

Starting materials for the synthesis of the GdCuGe sample were gadolinium ingots (Johnson Matthey), copper wire (Johnson Matthey, \varnothing 1 mm), and germanium lumps (Wacker), all with stated purities better than 99.9%. GdCuGe was prepared by arc-melting [20]. In a first step, small gadolinium pieces were arc-melted to buttons under argon (600 mbar). The argon was purified over titanium sponge (900 K), silica gel and molecular sieves. This pre-melting procedure strongly reduces a shattering during the strongly exothermic reactions with copper and germanium. The gadolinium button was then reacted with pieces of the copper wire and the germanium lump in the ideal 1:1:1 atomic ratio in the arc-melting crucible. The resulting button was remelted three times to ensure homogeneity. The total weight loss after the arc-melting procedures was less than 0.5%.

The purity of the sample was checked through a Guinier powder pattern using $\text{CuK}\alpha_1$ radiation and α -quartz ($a = 491.30$, $c = 540.46$ pm) as an internal standard. The Guinier camera was equipped with an image plate system (Fujifilm BAS-1800). The correct indexing of the pattern was facilitated by an intensity calculation [21] using the atomic parameters obtained from the structure refinement. The hexagonal lattice parameters (Table 1) were obtained by least-squares fit of the Guinier data. Our powder data compare well with the subcell data reported by Iandelli ($a = 424.1$, $c = 375.5$ pm) [16] and Mulder et al. ($a = 423.8$, $c = 376.0$ pm) [19]. No superstructure reflections indicating a doubling of the c parameter were observed on the powder patterns.

Table 1
Crystal data and structure refinement for GdCuGe (NdPtSb type, space group $P6_3mc$, $Z = 2$)

Empirical formula	GdCuGe
Molar mass	293.38 g/mol
Unit cell dimensions (Guinier data)	$a = 423.2(1)$ pm $c = 753.7(2)$ pm $V = 0.1169$ nm ³
Calculated density	8.34 g/cm ³
Crystal size	45 × 45 × 65 μm^3
Transm. ratio (max/min)	0.577/0.355
Absorption coefficient	49.4 mm ⁻¹
$F(000)$	250
θ range	5–45°
Range in hkl	± 8 , ± 8 , ± 14
Total no. reflections	3592
Independent reflections	414 ($R_{\text{int}} = 0.0538$)
Reflections with $I > 2\sigma(I)$	301 ($R_{\text{sigma}} = 0.0199$)
Data /parameters	414/10
Goodness-of-fit on F^2	1.147
Final R indices [$I > 2\sigma(I)$]	$R_1 = 0.0211$; $wR_2 = 0.0405$
R indices (all data)	$R_1 = 0.0318$; $wR_2 = 0.0443$
Flack parameter	0.25(13)
Extinction coefficient	0.011(1)
Largest diff. peak and hole	4.89 and -0.97 e/ \AA^3

Irregularly shaped single crystals of GdCuGe were obtained from the arc-melted sample by mechanical fragmentation. These crystals were first checked by Laue photographs on a Buerger precession camera (equipped with an image plate system, Fujifilm, BAS-1800) in order to establish their suitability for intensity data collection. Single crystal intensity data were collected at room temperature by use of a four-circle diffractometer (CAD4) with graphite monochromatized $\text{Mo-K}\alpha$ (71.073 pm) radiation and a scintillation counter with pulse height discrimination. Scans were taken in the $\omega/2\theta$ mode. An empirical absorption correction was applied on the basis of Ψ -scan data, followed by a spherical absorption correction. All relevant crystallographic data for the data collection and evaluation are listed in Table 1.

Although the X-ray powder data gave no hint for a doubling of the c -axis, the single crystal clearly showed these superstructure reflections. We have then collected intensity data for the doubled cell. The data set revealed 60 superstructure reflections with $I > 2\sigma(I)$. The seven strongest superstructure reflections (Miller index, F^2 value, standard uncertainty in parentheses) are: 015, 50.5(5.4); 027, 49.5(6.9); 017, 41.3(6.2); 01 $\bar{5}$, 40.6(5.4); $\bar{1}$ 3 $\bar{5}$, 35.8(4.9); $\bar{1}$ 3 $\bar{7}$, 31.0(5.5), and 013, 30.7(4.7).

Doubling of the c -axis for such an AlB_2 -related subcell can result in the ordering variants of the ZrBeSi type (space group $P6_3/mmc$ with ordered, planar hexagons), the NdPtSb type (space group $P6_3mc$), or the ScAuSi type (space group $P\bar{6}$; $m2$) [3]. Considering the results of the neutron diffraction on the terbium, dysprosium, holmium, and erbium compound, the ordering variant of the NdPtSb type [22] is most probable. We have then fixed the gadolinium site to 000 and the copper and germanium atoms were slightly shifted from the mirror planes at $z = 1/4$ and $3/4$ in the starting least-squares cycles. The refinement with SHELXL-97 (full-matrix least-squares on F^2) [23] with anisotropic atomic displacement parameters for all atoms fully confirmed the NdPtSb-type ordering and smoothly converged to the residuals listed in Table 1. Since the displacements of the copper (12σ) and germanium (4σ) atoms from the mirror planes are only small, the structure was also refined in the higher symmetry space group $P6_3/mmc$. These refinements, however, revealed extreme U_{33} values for these positions, this was also observed for the subcell refinement in $P6/mmm$, and consequently, the NdPtSb type ordering in space group $P6_3mc$ is the correct one. Although the powder patterns and the EDX data (see below) gave no hint for inhomogeneity, it might be possible that for some crystals of the sample a smaller degree of puckering might occur and those crystals might be better described with the ZrBeSi type.

Refinement of the correct absolute structure was ensured through refinement of the Flack parameter [24,25] (Table 1). A final difference electron-density synthesis was flat and did not reveal any significant residual peaks. The highest residual density was close to the gadolinium

Table 2
Atomic coordinates and isotropic displacement parameters (pm^2) for GdCuGe

Atom	Wyckoff site	x	y	z	U_{eq}
Gd	2a	0	0	0 ^a	64(1)
Cu	2b	2/3	1/3	0.7436(5)	100(4)
Ge	2b	2/3	1/3	0.2483(4)	72(2)

U_{eq} is defined as one third of the trace of the orthogonalized U_{ij} tensor.

^aThe z parameter of the gadolinium position was fixed at 0.

site and most likely resulted from an incomplete absorption correction. The results of the structure refinement are summarized in Table 1. The atomic coordinates and the interatomic distances are listed in Tables 2 and 3. Further information on the structure refinement is available.¹

The single crystal investigated on the four-circle diffractometer was analyzed using a LEICA 420 I scanning electron microscope with GdF₃, Cu, and Ge as standards. No impurity elements heavier than sodium were observed. The composition determined by EDX (34 ± 2 at% Gd; 33 ± 2 at% Cu; 33 ± 2 at% Ge) was in good agreement with the ideal 1:1:1 composition.

Heat capacity (C) measurements were performed on polycrystalline GdCuGe, by relaxation method using QD-PPMS. The sample was glued to calibrated HC-puck using Apizeon N grease. C was measured in the 3–50 K range with and without applied fields (H).

3. Results and discussion

3.1. Crystal chemistry

The unit cell of GdCuGe is presented in Fig. 1. The structure derives from the well-known AlB₂ type through an ordering of the copper and germanium atoms. The [Cu₃Ge₃] hexagons are slightly puckered and rotated by 60° around the c -axis within every other layer. Thus, GdCuGe is the germanide with the smallest puckering within the series of RECuGe germanides. Since full ordering within the [Cu₃Ge₃] hexagons of the RECuGe germanides with $RE = \text{La, Ce, Pr, Nd, Sm}$ is most likely the case, the latter germanides crystallize with the ZrBeSi or SrPtSb-type structures with planar hexagons rather than with a disordered AlB₂ type. For the various AlB₂ ordering variants we refer to a recent review article [3,4].

The Cu–Ge distances within the slightly puckered [Cu₃Ge₃] hexagons are 244 pm, only slightly larger than the sum of the covalent radii of 239 pm [26]. We can therefore assume significant Cu–Ge interactions. The slightly puckered [Cu₃Ge₃] layers are separated by the electropositive gadolinium atoms. The situation of chemical bonding in GdCuGe is similar to the REAuGe

Table 3
Interatomic distances (pm) in the structure of GdCuGe, calculated with the powder lattice parameters

Gd			
3	Cu		305.7
3	Ge		307.8
3	Ge		309.3
3	Cu		311.5
2	Gd		376.9
6	Gd		423.2
Cu			
3	Ge		244.4
3	Gd		305.7
3	Gd		311.5
Ge			
3	Cu		244.4
3	Gd		307.8
3	Gd		309.3

Standard deviations are equal or less than 0.2 pm. All distances of the first coordination spheres are listed.

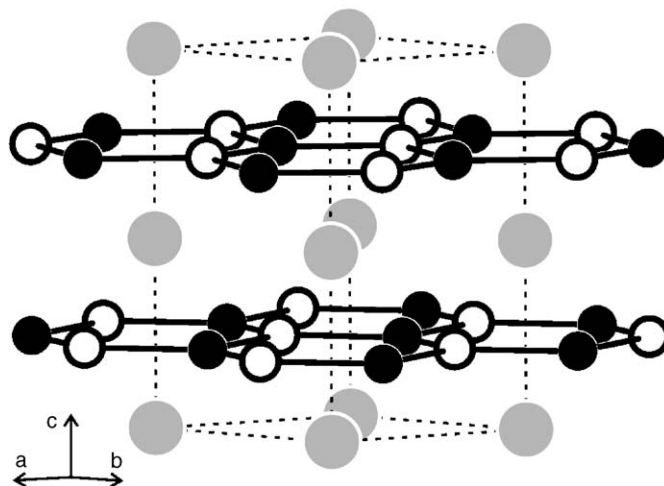


Fig. 1. Crystal structure of GdCuGe. The gadolinium, copper, and germanium atoms are drawn as medium gray, black filled, and open circles, respectively. The two-dimensional [CuGe] networks are emphasized.

germanides. For details we refer to these investigations [27,28].

3.2. Specific heat data

Fig. 2 shows the heat capacity behavior of GdCuGe measured under applied fields of 0, 10, 30 and 50 kOe. For $H = 0$, $C(T)$ measurement shows a broad peak like feature around 14 K (we thus refer this temperature as T_N), in consistence with the observation of antiferromagnetic ordering around 17 K determined by magnetic measurements, as per the literature reports [15–17]. Increasing H pushes the peak in $C(T)$ to lower temperatures, thus confirming the antiferromagnetic nature of the magnetic interactions in GdCuGe. An important observation we make here is the cross over of specific heat curves at two

¹Details may be obtained from: Fachinformationszentrum Karlsruhe, D-76344 Eggenstein-Leopoldshafen (Germany), by quoting the Registry No. CSD-416030.

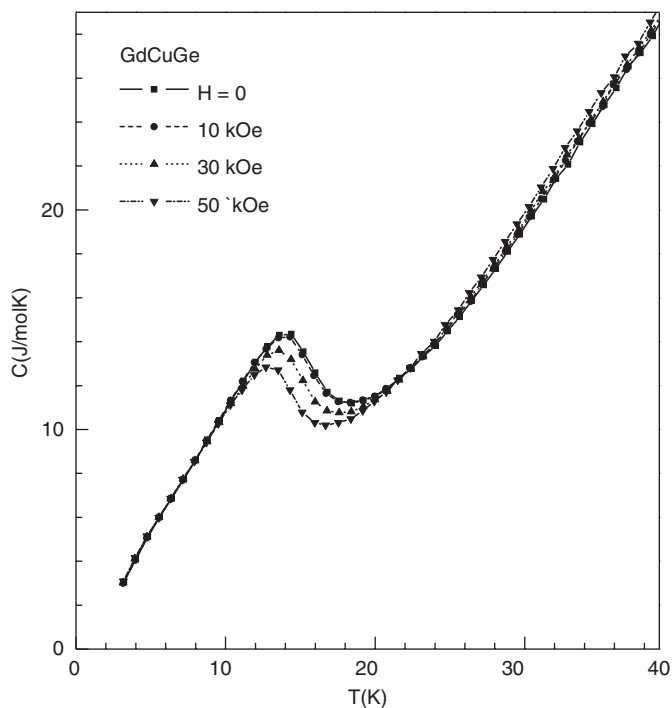


Fig. 2. Heat capacity (C) for GdCuGe measured as a function of temperature (T) at various applied fields (H).

definite points, which are also seen in case of many correlated systems such as ^3He , heavy fermion and Hubbard models [29]. The cross over of $C(T)$ curves for different H is more clearly visible in the plots of C/T vs. T shown in Fig. 3.

Within the Debye low-temperature approximation the measured specific heat is given as

$$C = \gamma T + \beta T^3 \text{ or } C/T = \gamma + \beta T^2, \quad (1)$$

where γ is the contribution from the conduction electron and β is the lattice contribution [30]. As per Eq. (1), the value of the γ is interpreted as the effective mass of electrons at the Fermi surface. *Heavy fermion* phenomenon is usually attributed to the unusual enhancement of γ value. However, due to the stable $4f$ shell of gadolinium, the mechanism such as f -electron hybridization or intermediate valence fluctuation are not applicable for explanation of such heavy-fermion-like-heat capacity behavior in gadolinium intermetallics.

In Fig. 3, we have plotted C/T vs. T^2 as insert. At low temperatures C follows the T^3 behavior (i.e., linear region in the C/T vs. T^2 plot) below 10 K up to 5 K. It should be noted here that the C/T vs. T^2 curve deviates below 5 K and drops sharply, indicating probably more complex magnetic behavior below 5 K. Such a behavior has been observed in other correlated systems also [31]. We have calculated the electronic coefficient of the heat capacity (also called the, γ) from the linear region of the C/T vs. T^2 curve in the ordered state. The γ value for the $H = 0$ measurement is of the order of 1 J/mol K^2 , which is similar to the values of γ in heavy fermion compounds. Though the explanation of

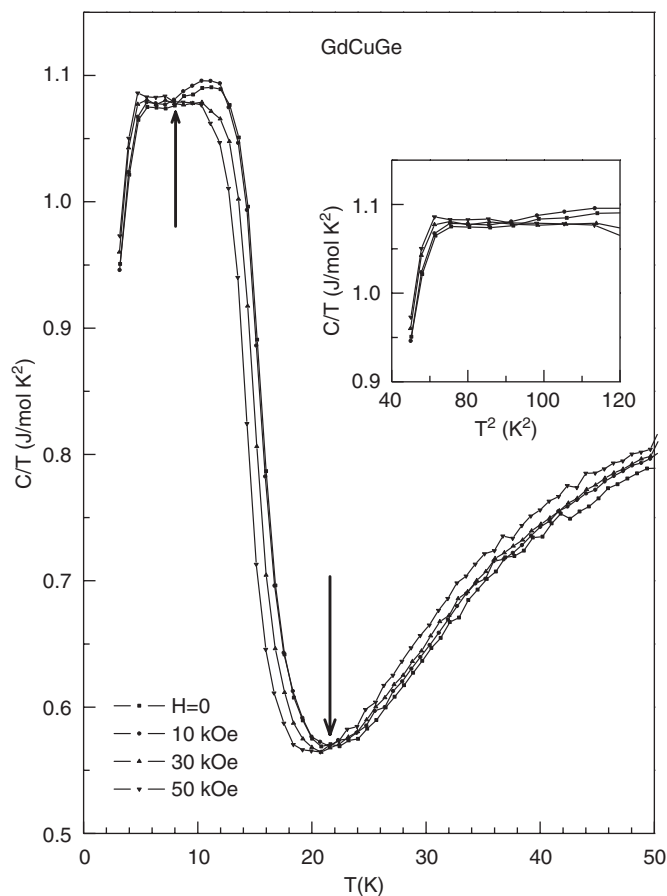


Fig. 3. Plot of C/T vs. T for GdCuGe measured under $H = 0, 10, 30$ and 50 kOe . The cross over of the heat capacity curves are indicated by vertical arrows. In the inset we have plotted C/T vs. T^2 , to highlight the linear region below $T = 10 \text{ K}$. See text for the details.

heavy fermions is not valid for Gd intermetallics, some Gd compounds have shown large γ values, indicating *heavy-fermion-like heat capacity* behavior [11,32,33].

In Fig. 4, we have plotted the variation of γ (in J/mol K^2). With increase in field, γ increases rapidly up to 30 kOe , and then increases marginally for 50 kOe . This can be understood by the fact that in hexagonal gadolinium alloys, magnetoelastic effects are connected with a highly anisotropic coupling between gadolinium moments [34].

The specific heat measured under different fields crosses each other due to the change of entropy with respect to field. In Fig. 5, we show the total entropy for GdCuGe, calculated from $C(T)$ measured under different fields. For gadolinium (S-state ion with zero angular momentum and $J = 7/2$) the full magnetic entropy ($R \ln 8$) should be recovered just above the ordering temperature. But for GdCuGe, the total entropy (S) is not saturated above T_N but increases up to the highest temperature measured, i.e., 50 K without any signature of saturation. In Fig. 6 we show the difference in entropies measured at different H . ΔS changes sign from negative to positive at lower temperatures ($T < T_N$) for higher fields, as seen in magnetic

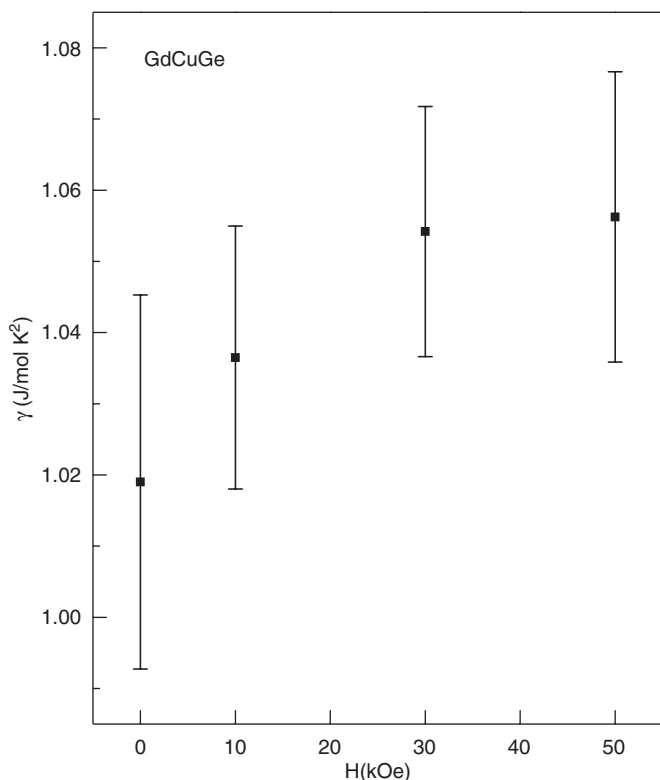


Fig. 4. Variation of the electronic coefficient of heat capacity (γ) under applied fields (H).

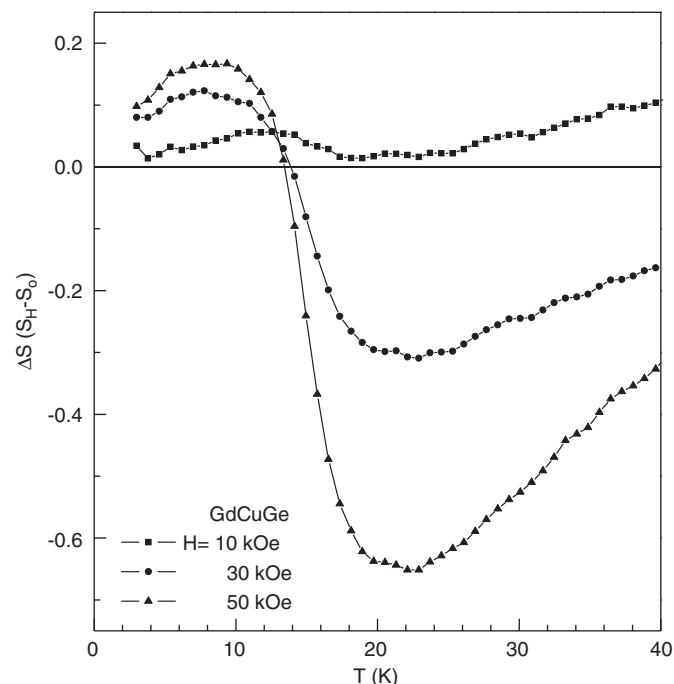


Fig. 6. Difference in total entropy (ΔS) of GdCuGe measured in applied field and zero field. S_H is the entropy in field H and S_0 is the total entropy when $H = 0$.

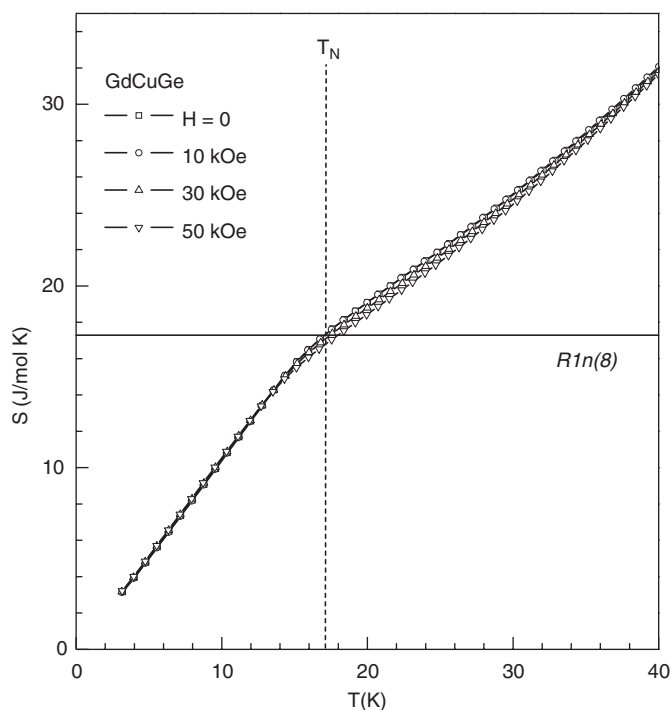


Fig. 5. Field dependence of total entropy (S) vs. T for GdCuGe calculated from C measured at $H = 0, 10, 30$ and 50 kOe. The vertical line indicates the anti-ferromagnetic ordering temperature (T_N), whereas the horizontal line is drawn to show the value of full magnetic entropy for Gd ($R\ln(2J+1)$ for $J = 7/2$).

transformations [35]. The plot of ΔS also indicates that GdCuGe shows very weak magnetocaloric effect [36].

4. Conclusions

A single crystal study clearly confirmed copper-germanium ordering for GdCuGe within the NdPtSb-type model. GdCuGe exhibits heavy-fermion-like heat-capacity anomalies, with large gamma value and cross-over of $C(H, T)$ curves. The crossing of $C(T)$ curves in ^3He , heavy fermions and Hubbard models takes place precisely at one or two temperatures [29]. In the case of GdCuGe, $C(H, T)$ crosses at two temperatures, below (~ 8 K) and above (~ 21 K) T_N , which is quite interesting, since gadolinium intermetallics are not expected to show the heavy fermion phenomenon. Comparison of heat capacities of GdCuGe with isotopic compounds such as Gd_2CuGe_3 and GdCu_2Ge_2 indicates that the heat-capacity features in these gadolinium compounds are possibly governed by the amplitude modulation of magnetic structure [32,33,37–39]. The present study hence contributes to the ongoing search for gadolinium intermetallic compounds exhibiting novel magnetic properties.

Acknowledgments

We thank H.-J. Göcke for the work at the scanning electron microscope and Dipl.-Ing. U.Ch. Rodewald for the intensity data collection. This work was supported by the Deutsche Forschungsgemeinschaft through SPP 1166 *Lanthanoidspezifische Funktionalitäten in Molekül und*

Material. C.P. Sebastian and S. Rayaprol are indebted to the NRW Graduate School of Chemistry and the Alexander von Humboldt-Stiftung for research grants.

References

- [1] A. Szytuła, J. Leciejewicz, Handbook of Crystal Structures and Magnetic Properties of Rare Earth Intermetallics, CRC Press, Boca Raton, FL, 1994.
- [2] K.A. Gschneidner Jr., L. Eyring, (Eds.), Handbook on the Physics and Chemistry of Rare Earths, vols. 1–34, 1978–2005 (Chapters 48, 51, 156, 164, 173–175, 207, 212, 218).
- [3] R. Pöttgen, D. Johrendt, Chem. Mater. 12 (2000) 875.
- [4] R.-D. Hoffmann, R. Pöttgen, Z. Kristallogr. 216 (2001) 127.
- [5] R. Mallik, E.V. Sampathkumaran, Phys. Rev. B 58 (1998) 9178.
- [6] V.K. Pecharsky, K.A. Gschneidner Jr., Phys. Rev. Lett. 78 (1997) 4494.
- [7] A.M. Tishin, Yu.S. Spichkin, The Magnetocaloric Effect and its Applications, IOP Publishing Ltd., Bristol, 2003.
- [8] K. Sengupta, K.K. Iyer, E.V. Sampathkumaran, Phys. Rev. B 72 (2005) 54422.
- [9] E.V. Sampathkumaran, R. Malik, in: A. Hewson, V. Zlatic, (Eds.), Concepts in Correlation, vol. 110, Kluwer, Dordrecht, 2003, p. 666; cond-mat/0211625.
- [10] E. Brück, J. Phys. D: Appl. Phys. 38 (2005) R381.
- [11] A.N. Chaika, A.M. Ionov, M. Busse, S.L. Molodtsov, S. Majumdar, G. Behr, E.V. Sampathkumaran, W. Schneider, C. Laubschat, Phys. Rev. B 64 (2001) 125121.
- [12] K. Łątka, R. Kmieć, A.W. Pacyna, Th. Fickenscher, R.-D. Hoffmann, R. Pöttgen, J. Magn. Magn. Mater. 280 (2004) 90.
- [13] F. Canepa, M.L. Fornasini, F. Merlo, M. Napolitano, M. Pani, J. Alloys Compd. 312 (2000) 12.
- [14] W. Rieger, E. Parthé, Monatsh. Chem. 100 (1969) 439.
- [15] S. Baran, A. Szytuła, J. Leciejewicz, N. Stüsser, A. Zygmunt, Z. Tomkowicz, M. Guillot, J. Alloys Compd. 243 (1996) 112.
- [16] A. Iandelli, J. Alloys Compd. 198 (1993) 141.
- [17] S. Baran, A. Szytuła, J. Leciejewicz, N. Stüsser, A. Zygmunt, Z. Tomkowicz, M. Guillot, Physica B 234–236 (1997) 656.
- [18] H. Oesterreicher, Phys. Stat. Sol. A 39 (1977) K75.
- [19] F.M. Mulder, R.C. Thiel, K.H.J. Buschow, J. Alloys Compd. 205 (1994) 169.
- [20] R. Pöttgen, T. Gulden, A. Simon, GIT Labor-Fachzeitschrift 43 (1999) 133.
- [21] K. Yvon, W. Jeitschko, E. Parthé, J. Appl. Crystallogr. 10 (1977) 73.
- [22] G. Wenski, A. Mewis, Z. Kristallogr. 176 (1986) 125.
- [23] G.M. Sheldrick, SHELXL-97, Program for Crystal Structure Refinement, University of Göttingen, Germany, 1997.
- [24] H.D. Flack, G. Bernadinelli, Acta Crystallogr. A 55 (1999) 908.
- [25] H.D. Flack, G. Bernadinelli, J. Appl. Crystallogr. 33 (2000) 1143.
- [26] J. Emsley, The Elements, Clarendon Press, Oxford, 1989.
- [27] R. Pöttgen, H. Borrmann, C. Felser, O. Jepsen, R. Henn, R.K. Kremer, A. Simon, J. Alloys Compd. 235 (1996) 170.
- [28] W. Schnelle, R. Pöttgen, R.K. Kremer, E. Gmelin, O. Jepsen, J. Phys. C 9 (1997) 1435.
- [29] D. Vollhardt, Phys. Rev. Lett. 78 (1997) 1307.
- [30] E.S.R. Gopal, Specific Heats at Low Temperatures, Plenum, New York, 1966.
- [31] S. Rayaprol, E.V. Sampathkumaran, Phys. Rev. B 71 (2005) 94403.
- [32] E.V. Sampathkumaran, I. Das, Physica B 223&224 (1996) 149.
- [33] S. Majumdar, E.V. Sampathkumaran, Phys. Rev. B 61 (2000) 43.
- [34] E. Gratz, A. Lindbaum, J. Magn. Magn. Mater. 177–181 (1998) 1077.
- [35] J.G. Sereni, Encyclopedia of Materials: Science and Technology, Elsevier Publishers, Amsterdam, ISBN 0-08-0431526, 2001, pp. 4986–4994.
- [36] K.A. Gschneidner Jr., V.K. Pecharsky, Annu. Rev. Mater. Sci. 30 (2000) 387.
- [37] J.A. Blanco, D. Gignoux, P. Morin, D. Schmitt, Europhys. Lett. 15 (1991) 671.
- [38] J.A. Blanco, D. Gignoux, D. Schmitt, Phys. Rev. B 43 (1991) 13145.
- [39] M. Rotter, M. Loewenhaupt, M. Doerr, A. Lindbaum, H. Michor, Phys. Rev. B 64 (2001) 14402.